CrossMark

ORIGINAL PAPER

Novel preparation of sensitized ZnS nanoparticles and its use in photocatalytic degradation of tetracycline

M. Ahadi[1] · M. Saber Tehrani[1] · P. Aberoomand Azar[1] · S. Waqif Husain[1]

Abstract Sensitized ZnS nanoparticles were synthesized by chemical precipitation method using anthocyanin as the capping agent and sensitizer. X-ray diffractometer, field-emission scanning electron microscope, transmission electron microscopy, UV visible spectrophotometer, Fourier transform infrared spectroscopy and photoluminescence spectrometry methods were used for the characterization of nanoparticles. The electron microscopy studies of nanoparticles showed that the size of crystallites is in the range of 35–80 nm and optical studies showed a blue shift in the absorption edge by adding capping agent. The effective band gap energy was increased with decrease in the particle size. Photocatalytic activities of sensitized ZnS and pure ZnS were evaluated by degradation of tetracycline in aqueous solution under visible light irradiation, and progress of the reaction was monitored spectrophotometrically. The different parameters affecting degradation such as the pH of solution, amount of semiconductor and reusability of catalyst for three cycles and the photocatalytic degradation kinetics of tetracycline were studied. More than 80% degradation was achieved within 5 h under visible light.

Keywords Anthocyanin · Capping agent · Chemical oxygen demand (COD) · Degradation efficiency · Sensitizer

✉ M. Saber Tehrani
  drmsabertehrani@yahoo.com

[1] Department of Chemistry, Faculty of Science, Science and Research Branch, Islamic Azad University, Tehran, Iran

Introduction

There is present an increasing concern, about penetration of pharmaceuticals into the environment and the related risks (Kummerer 2009). This is caused, by a very high consumption of drugs by societies in different countries. Tetracycline (TC) is one of the most widely used antibiotics in aquaculture and veterinary medicines (Palominos et al. 2009). It is excreted via feces and urine, because of its poor absorption. The most dangerous effect of antibiotics in the environment is the development of multi-resistant bacterial strains that can no longer be treated with the present known drugs (Addamo et al. 2005). Hence, the occurrence, fate and behavior of antibiotics in the environment have attracted growing concern of scientific interest (Verma et al. 2007). Significant amount of TC have been detected in superficial, potable water and sludge due to their ineffective removal by the conventional water treatment methods. Since traditional biological methods could not effectively eliminate antibiotics, there is a demand of effective techniques for rapid degradation of TC in the environment (Bautitz and Nogueira 2007).

Over the past decade, many research efforts have been devoted around the world to develop a new, more powerful, and very promising technique called advanced oxidation processes (AOPs) to treat the contaminants in drinking water and industrial effluents. AOPs are capable of degrading contaminants at ambient temperature and pressure and have an advantage over biological treatment of waste streams containing toxic or bio-inhibitory contaminants. The central attraction of advanced oxidation processes is that organic contaminants are commonly oxidized to CO_2 (Muruganandham et al. 2014). AOPs can be classified into two main groups: (1) non-photochemical AOPs and (2) photochemical AOPs. Non-photochemical AOPs

Springer

include cavitation (Adewuyi 2001), Fenton (Masarwa et al. 2005), zonation at high pH (Ensing et al. 2003), ozone/hydrogen peroxide (Tehrani-Bagha et al. 2010), wet air oxidation (Arslan-Alaton and Ferry 2002), etc. Photochemical oxidation processes include homogenous processes such as vacuum UV photolysis (Gonzaleza et al. 2004), UV/H_2O_2 (Dein et al. 2003), UV/O_3 (Peyton and Glaze 1988) and heterogeneous photocatalysis processes. Heterogeneous photocatalysis is one of the AOPs and is based on the direct or indirect absorption of photons from ultraviolet (UV) or visible light by a semiconductor that possesses the appropriate energy gap. The semiconductor for the photocatalysis should be chemical or biological, inert, stable, inexpensive, easy to synthesis and its production without human and environmental risks. There are many known semiconductors which could be used for this purpose such as TiO_2, ZnO, ZrO_2, V_2O_5, WO_3, Fe_2O_3, SnO_2, CdSe, GaP and metal sulfides (CdS and ZnS).

Transition metal sulfides, in particular ZnS, have unique catalytic functions as a result of the rapid generation of electron–hole pairs by photo excitation. Their highly negative reduction potentials of excited electrons could be compared to those of TiO_2 and ZnO (Zhao et al. 2007). But it has a large band gap energy (3.68 for bulk) and absorbs radiation of wavelengths lower than 400 nm, corresponding to the UV region. To overcome this limitation, it is necessary to increase the absorbance of the visible light by photocatalysts using metal doping (Chauhan et al. 2014; Chen et al. 2012; Kim et al. 2003; Singla et al.2016; Sivakumar et al. 2014; Yang et al. 2001, 2003), coupling with small band gap semiconductors such as CdS and CuS (Thuy et al. 2014; Zhang et al. 2011) and sensitization with polymers, metal complexes, organic or natural dyes (Chen et al. 2009; Zhiyu et al. 2006). Organic dye sensitization has been widely used to enable visible light absorbing by wide band gap semiconductors such as TiO_2 (Pei and Luan 2012). This paper reports a simple route for the preparation of sensitized ZnS nanoparticles via the chemical precipitation method. To prevention of water pollution resulted of organic dyes, natural dyes such as anthocyanin extracted from rose flowers was used as a sensitizer. Anthocyanin was selected for the study due to its low cost, availability, easily extraction and applicability without additional purifications. It has several carbonyls and hydroxyl groups so it can easily anchor to the semiconductor surface. All these reasons make anthocyanin vital alternative to synthetic dyes and even most of other natural dyes. Another role of anthocyanin is a capping agent to inhibit nanoparticle overgrowth and aggregation. The prepared nanoparticles were characterized and then utilized as photocatalysts in the photo degradation of TC solution. In this study, preparation and degradation procedure of ZnS

nanoparticles were performed in winter 2015 at Medical Branch of Islamic Azad University and characterization of nanoparticles was carried out in spring 2016 in faculty of electrical of Tehran University and Science and Research Branch of Islamic Azad University.

Materials and methods

The tetracycline antibiotics selected for this study were from Sigma-Aldrich. Ethanol and other materials such as NaOH, HCl, Na_2S, $ZnSO_4$, H_2SO_4, K_2CrO_4, $HgSO_4$, $(NH_4)_2Fe(SO_4)_2 \cdot 6H_2O$ were from Merck (Germany). Anthocyanin dye was extracted from rose flowers. The pH values were measured by a pH meter (Metrohm744). A centrifuge (Hettich, ROTOFIX 32A, 6000 RPM) was used for separation of nanoparticles from solution. The progress of photocatalytic degradation was monitored by chemical oxygen demand (COD) analysis which was measured by the dichromate reflux method (Westwood D 2007). The concentration of the sample solutions was measured by UV–Vis spectrophotometer (Varian Cary 300). UV–Vis reflectance spectrophotometer (color-eye 7000A-xrite) was used to analyze light reflectance of photocatalysts. The FT-IR spectra of photocatalysts were recorded with a Thermo Nicolet (NEXUS ESP 870). Photoluminescence (PL) study was carried out using a fluorescence spectrophotometer (PerkinElmer LS 55) with an excitation wavelength of 220 nm. The morphology and size distribution of the photocatalyst nanoparticles were determined by field-emission scanning electron microscopy (FESEM) (ZEISS-Sigma) and transmission electron microscopy (TEM) (cm30 Philips). The X-ray diffraction studies of the samples were carried out on a SEIFERT X-ray diffractometer with the Cu-Kα radiation ($\lambda = 1.54$ Å) at 40 kV and 30 mA with a scanning rate of 3°/min (from $2\theta = 20°$–80°).

Irradiation source

The degradation was carried out using a 650 W halogen lamp as the visible light source (Osram lamp, Germany).

Anthocyanin dye extraction

The anthocyanin was extracted from red rose flowers according to the methodology of Lees and Francis (Vanini et al. 2009). Five grams of red rose flowers were cut to small pieces and soaked in 100 mL ethanol, acidified with 0.1% hydrochloric acid at a constant temperature about 40 °C for 30 min and the extracted dye was filtered. Then deep red solution was stored in a dark color glass flask for further use.

Nanoparticle preparation

In a typical synthesis, 5 mmol of zinc sulfate was dissolved in 25 mL deionized water then mixed with 25 mL of the extracted anthocyanin dye. 75 mL of 0.2 M sodium sulfide was added dropwise into the reaction mixture, while it was stirred vigorously for 2 h. White precipitate of ZnS was formed during the reaction. When the pH is raised to basic pH, anthocyanin will be absorbed by sediment. The green gel solution was centrifuged at 6000 rpm for 5 min. Then, it was washed with ethanol and deionized water several times to remove unreacted dye and impurities. The precipitate was then dried in an oven at 80 °C for 6 h. A green powder of ZnS was obtained.

Degradation procedure

The degradation of TC in the presence of sensitized ZnS was studied using a 650 W halogen lamp as the visible light source. 200 mg of the photocatalyst was added to 100 mL TC solution (40 mg L^{-1}), and the suspension was magnetically stirred during irradiation. The reaction mixture was exposed to visible irradiation directly coming out from the source lamp (adjusted directly above the reaction mixture). At regular intervals, approximately 3 mL of sample was collected and centrifuged at 6000 rpm for 5 min in order to remove the solid particles and then the liquid phase was removed out for analysis of the remaining contaminant at 356 nm. To determine the photocatalytic degradation percent, the following equation was used (Eq. 1).

$$\text{Degradation }\% = (A_0 - A_t/A_0) \times 100 \tag{1}$$

where A_0 is the absorbance at $t = 0$ h and A_t is the absorbance at time t (h).

Results and discussion

Structural and morphological characterization

The XRD pattern of pure ZnS (bulk) shows three main peaks at the scattering angles 28.8°, 48°, 56.8°, which are ascribed to the (111), (220), and (311) crystal planes of ZnS NPs, respectively (Fig. 1). All the diffraction peaks were in agreement with the standard data of cubic-type ZnS (JCPPS card NO. 05-0566). Pure ZnS peaks are quite short because of amorphous component. The XRD of sensitized ZnS exhibited both sharper and broader features implying lower agglomeration and size reduction. Moreover, the crystallinity of sensitized ZnS was improved without any change in the cubic phase.
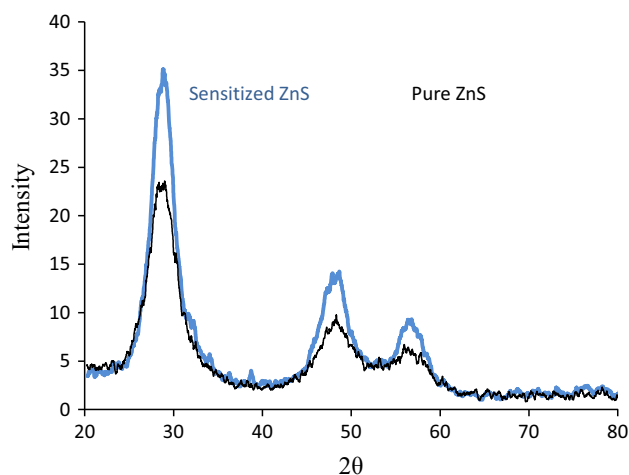

Fig. 1 XRD pattern of pure ZnS and sensitized ZnS NPs

The FESEM and TEM have been used to characterize the size, shape and morphology of the formed nanoparticles. Figure 2 shows electron microscopy images of the pure and sensitized ZnS NPs. These images demonstrate that anthocyanin plays important role on morphology and reduced size of NPs and also show that particle agglomeration was effectively inhibited by the introduction of the anthocyanin on the semiconductors surface. The size of the obtained sensitized ZnS nanoparticles was in the range of 35–80 nm.

FT-IR spectra of the anthocyanin, pure ZnS and sensitized ZnS particles are shown in Fig. 3. The characteristic major peaks of pure ZnS can be observed at about 1113, 1000 and 617 cm^{-1}, which are in good agreement with the reported results in references (Kuppayee et al. 2011; RemaDevi et al. 2007). The observed peak at 1625 cm^{-1} is assigned to the C=O stretching mode of CO_2, and also a broad absorption peak at 3000–3600 cm^{-1} is corresponded to O–H stretching mode arising from the absorption of water on the surface of nanoparticles. Location of the sensitized ZnS peaks due to anthocyanin adsorption has changed. The observed peak at 1188 cm^{-1} is assigned to the C–O stretching mode of anthocyanin molecule. But the spectra does not show any broad absorption peak at 3000–3600 cm^{-1} corresponded to O–H stretching mode arising from the absorption of water on the surface of ZnS nanoparticles and O–H stretching mode arising from anthocyanin molecule because of new bond between anthocyanin molecules and ZnS nanoparticles (1057 cm^{-1}).

The photoluminescence spectra (PL) of sensitized ZnS and pure ZnS with 220 nm excitation wavelength are shown in Fig. 4. The photoluminescence of sensitized ZnS with a peak at 300 nm corresponding to band gap emission and emission peak at 570 nm associated with structural defects. The band gap emission is blue shifted from the bulk band gap emission of pure ZnS at 320 nm due to the
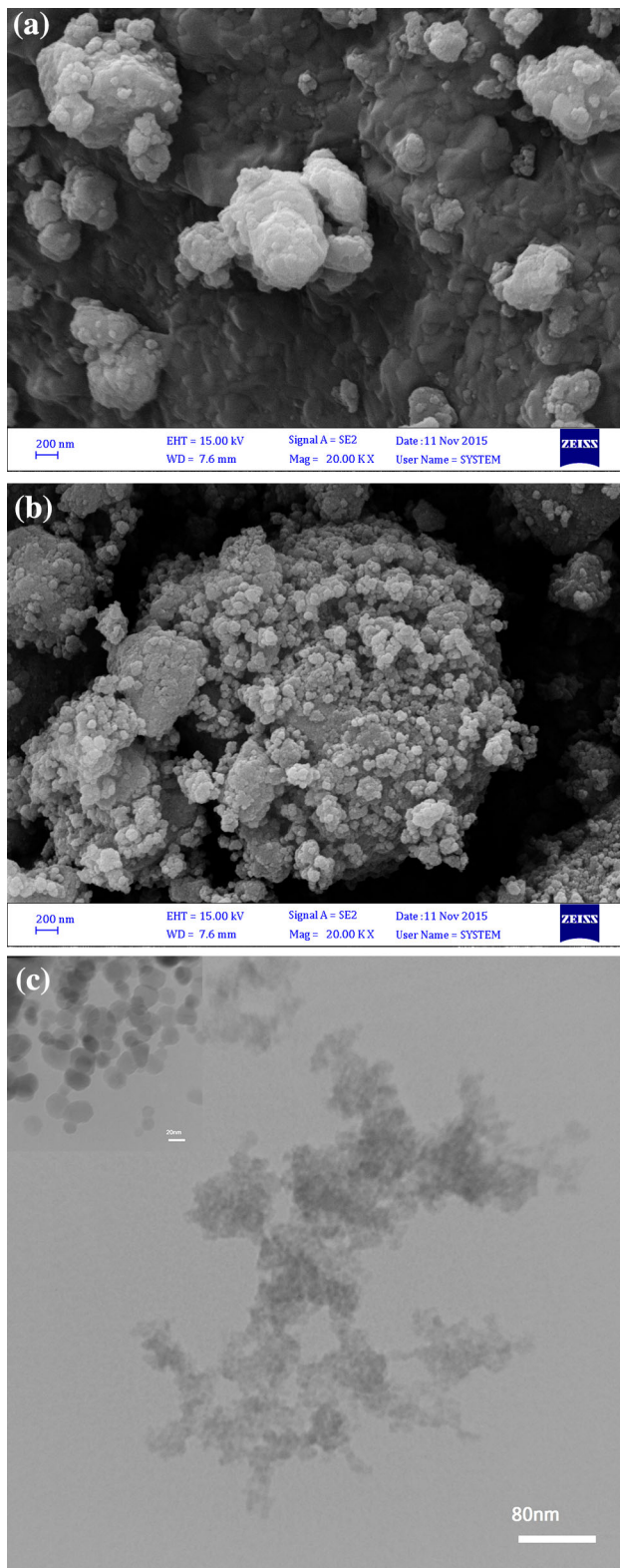
Fig. 2 FE-SEM of pure ZnS (bulk) (**a**), FE-SEM of sensitized ZnS (**b**), TEM of sensitized ZnS (**c**)

small size of the sensitized ZnS in comparison with pure ZnS. The wide emission peak around 400 nm was attributed to photoluminescence of anthocyanin. Energy band gap was calculated using Eq. 2.

$$E_g(ev) = 1240/\lambda(nm) \qquad (2)$$

where λ is the wavelength (nm) of PL peak. Calculated band gap according to the formula of pure ZnS (emission peak at 320 nm) and sensitized ZnS (emission peak at 300 nm) were obtained 3.8 and 4.1 eV, respectively.

The pure ZnS and sensitized ZnS nanoparticles were dispersed in deionized water for optical tests (Fig. 5). The UV–visible absorption spectra of these samples have been recorded in the range of 200 to 800 nm as shown in Fig. 5a. The absorption peaks were observed around 298 and 266 nm corresponding to pure ZnS and sensitized ZnS, respectively. The absorption peaks of sensitized ZnS are considerably blue-shifted compared to that of pure ZnS. By reducing the size of sensitized ZnS nanoparticles, a change in band gap energy of nanoparticles was seen. Moreover, reflection results reveal that sensitized ZnS has a good absorption for UV and Visible light in the wavelength range of 200–650 nm compared with pure ZnS (200–350 nm) (Fig. 5b).

The direct band gap energy can be estimated from a plot of $(\alpha h v)^2$ vs photon energy ($h v$) (Eq. 3):

$$(\alpha h v)^2 = A(h v - E_g) \qquad (3)$$

where $h v$: photon energy, α: absorption coefficient, E_g: energy band gap, A: constant. The value of direct band gap was determined by extrapolating the straight line portion of $(\alpha h v)^2$ versus $h v$ graph to the $h v$ axis as shown in Fig. 6. The results shows that band gap energies of pure (bulk) and sensitized ZnS were 3.8 and 4.1 eV, respectively, which corresponded to calculated band gap energy from photoluminescence. This change in band gap energy of nanoparticles was due to reducing the size of sensitized ZnS nanoparticles.

Photocatalytic degradation of tetracycline (TC)

The effect of sensitized ZnS and pure ZnS nanoparticles as photocatalyst under visible light in degradation of TC is shown in Fig. 7a. The photocatalytic degradation of TC was followed at λ_{max} of 356 nm. About 81% of TC was photocatalytically degraded within 5 h with the presence of sensitized ZnS under visible light irradiation. For sensitized ZnS in the absence of light, degradation was not obtained and decrease in concentration of TC occurs due to poor adsorption onto the surface of nanoparticles. The pure ZnS absorbs only UV irradiation. Thus, degradation efficiency

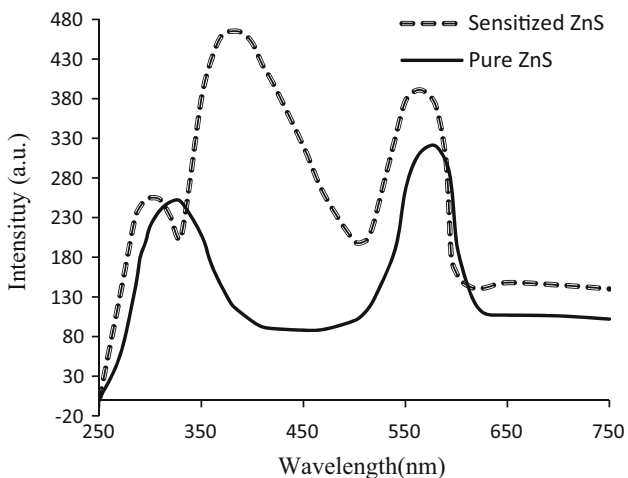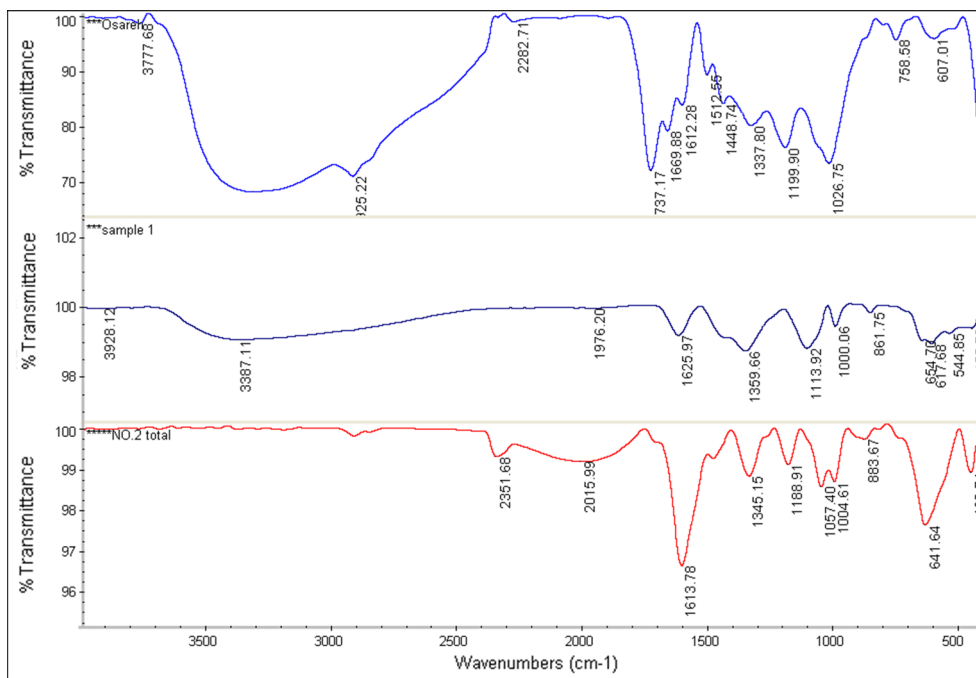**Fig. 3** FTIR spectra of anthocyanin, pure ZnS, sensitized ZnS

Fig. 4 The PL spectra of sensitized ZnS and pure ZnS with 220 nm excitation wavelength

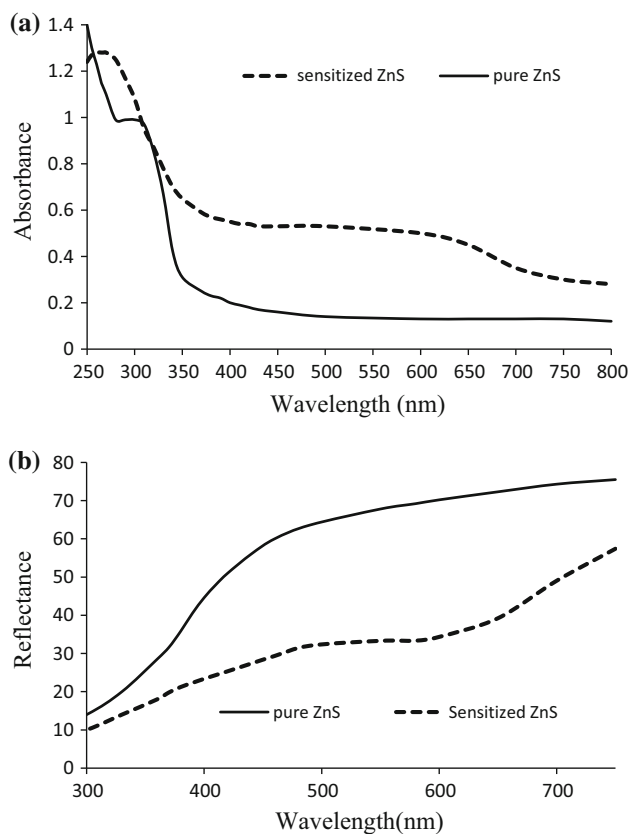**Fig. 5 a** UV–Vis absorbance spectra of pure ZnS and sensitized ZnS. **b** UV–Vis reflectance spectra of pure ZnS and sensitized ZnS

is very low under visible light irradiation. Sensitized ZnS is more efficient in the degradation of TC compared to pure ZnS. In the process of photodegradation, the anthocyanin excited by visible light and the excited electrons in the dye molecule LUMO moves to the conduction band of ZnS. The photogenerated electrons react with O_2 adsorbed on the ZnS surface, reducing it to superoxide radical anion $O_2^{-\cdot}$. The photogenerated holes react with OH^- or H_2O, oxidizing them to $OH^\cdot$ radicals. The $OH^\cdot$ radical and

2802

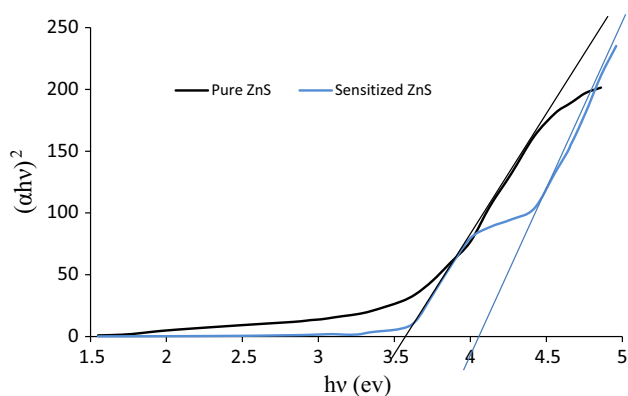Int. J. Environ. Sci. Technol. (2016) 13:2797–2804
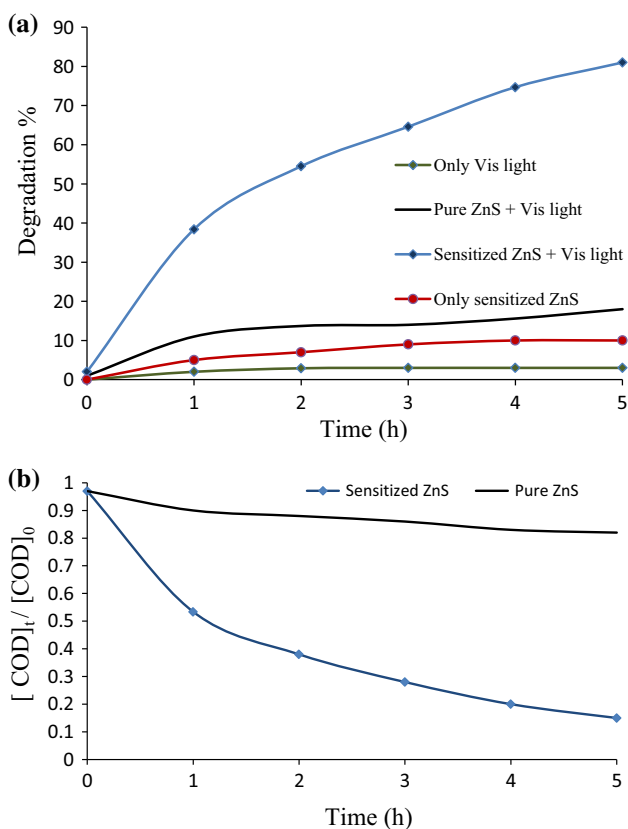

Fig. 6 $(\alpha h v)^2$ against *hv* plots of sensitized ZnS

Fig. 7 a The degradation curves of TC solution under visible light, **b** the ratio of $[COD]_t/[COD]_o$ versus time (TC: 40 mg L^{-1}, pH 7, sensitized ZnS NPs: 200 mg)

$[COD]_t/[COD]_o$ for a given concentration 40 mg L^{-1} of TC is shown in Fig. 7b. $[COD]_o$ and $[COD]_t$ are the chemical oxygen demand values before and after degradation at time *t* (h), respectively. More than 50% of TC degraded in less than an hour.

Effective parameters in degradation

Influence of the pH

Effect of pH on the catalyst efficiency in TC degradation has been investigated using sensitized ZnS under visible light. Sensitized ZnS is not stable at pH < 6 and more than 10. So the effect of pH has been studied at pH range of 6–10. The pH of TC solution (40 mg L^{-1}) is approximately 6. The 0.01 M NaOH has been used for adjusting pH of TC solution. At high pH (pH > 8), absorption wavelength shows red shift and degradation efficiency is reduced. It could be attributed to the higher stability of TC solution at basic pH. The results indicate that the degradation of TC was best achieved in a solution of pH 7.

Effect of amount of semiconductor

Figure 8 shows the degradation efficiency of 40 mg L^{-1} TC solution by different amounts of sensitized ZnS between 2.5 and 500 mg. The photocatalytic process was carried out using the procedure established previously. The result indicates that increasing the amount of nanoparticles up to 150 mg, increases the degradation efficiency due to the enhancement in the availability of active sites. Higher amounts of photocatalyst up to 300 mg show no change in efficiency; at higher concentration of photocatalyst (>300 mg), the photocatalytic process was inefficient due to aggregation of NPs (reducing the contact between the
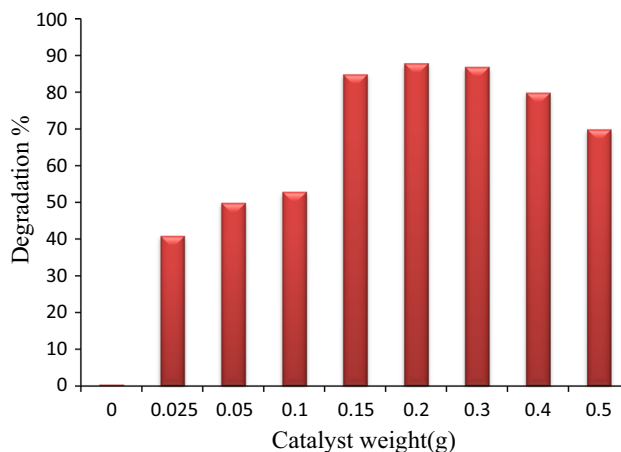
remaining holes in the valence band of the anthocyanin could oxidize most organic contaminations to the mineral end products (Pei and Luan 2012).

Chemical oxygen demand (COD) values have been related to the total concentration of TC in the solution so it was determined by the standard method (using a strong oxidizing agent potassium dichromate, sulfuric acid, and silver sulfate as a catalyst) (Westwood 2007). The ratio of

Fig. 8 Effect of amount of semiconductor on photocatalytic degradation efficiency (TC: 40 mg L^{-1}, pH 7, 5 h)

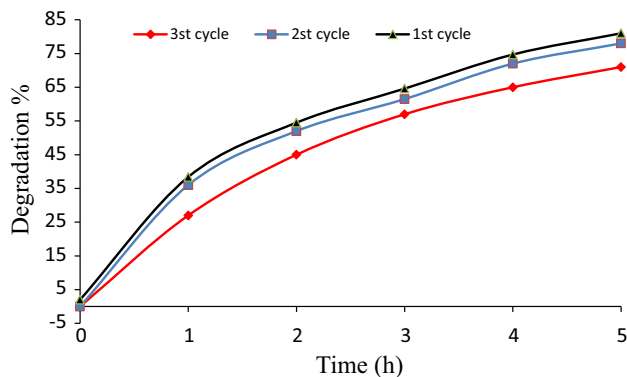**Fig. 9** Effect of reusability of photocatalyst (TC: 40 mg L^{-1}, pH 7, sensitized ZnS NPs: 200 mg)

Fig. 10 Kinetic studies for photo catalytic degradation of TC solution (TC: 40 mg L^{-1}, pH 7, sensitized ZnS NPs: 200 mg)

catalyst and the reaction mixture) and high turbidity of mixture (more light scattering) (San et al. 2001).

Recycling of the photocatalyst

To check the reusability of the photocatalyst, degradation of TC was carried out under optimized and similar conditions for three cycles and the results are shown in Fig. 9. For each new cycle, the degraded TC solution containing catalyst was centrifuged at 6000 rpm for 5 min and it was washed several times with distilled water and then dried at 80 °C for 60 min. For the three successive experiments, the rates of degradation of TC were 81, 78, and 71%, respectively, within 5 h. The photocatalyst could be used for three cycles with minimal change in catalyst property and degradability.

Kinetics study of degradation

The photocatalytic degradation of tetracycline was observed to the pseudo first-order decay kinetics Eq. 4:

$$\ln(C_0/C) = kt \tag{4}$$

where k is the rate constant of the reaction, C is the reactant concentration in the reaction time, and C_0 is the initial concentration of reactant.

The pseudo first-order degradation curves are depicted in Fig. 10, A plot of ln (C_0/C) shows a linear relationship with the irradiation time where the slope equals the rate constant (k). The values of R^2 were 0.9924 for sensitized ZnS and 0.9864 for pure ZnS. The calculated rate constant (k) for sensitized ZnS was 0.3157 min^{-1}, and rate constant for pure ZnS was 0.0327 min^{-1}. It is clear that the pure ZnS shows lower photo degradation efficiency of TC as compared to the sensitized ZnS under visible light. The increased rate constant for sensitized ZnS is due to the additional visible light absorption by anthocyanin and
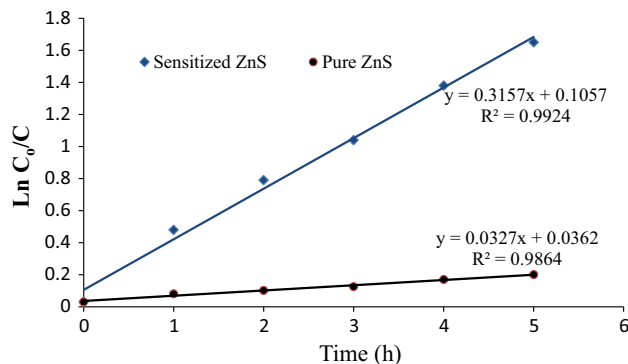
electron transfer from anthocyanin to the conduction band of ZnS and reducing recombination of electron–hole pair.

Conclusion

In this work, a chemical precipitation method for the fabrication of sensitized ZnS nanoparticles using anthocyanin as a sensitizer and capping agent has been developed. The sensitized ZnS nanoparticles show higher photocatalytic performance for the degradation of TC solution compared to pure ZnS under visible light. The influences of different factors on the degradation, recyclability of the photocatalyst and the rate of degradation have been studied. These results suggest that sensitized ZnS NPs in the presence of sunlight may be used as a very suitable and simple method for treatment of waste waters in textile and pharmaceutical industries.

References

Addamo M, Augugliaro V, Paola A, García-López E, Loddo V, Marcì G, Palmisano L (2005) Removal of drugs in aqueous systems by photoassisted degradation. J Appl Electrochem 35:765–774

Adewuyi YG (2001) Sonochemistry: environmental science and engineering applications. Ind Eng Chem Res 40:4681–4715

Arslan-Alaton I, Ferry JL (2002) Application of polyoxotungstates as environmental catalysts: wet air oxidation of acid dye orange II. Dyes Pigm 54:25–36

Bautitz IR, Nogueira RFP (2007) Degradation of tetracycline by photo-Fenton process solar irradiation and matrix effects. J Photochem Photobiol, A 187:33–39

Chauhan R, Kumar A, Chaudhary RP (2014) Photocatalytic degradation of methylene blue with Cu doped ZnS nanoparticles. J Lumin 145:6–12

2804

Int. J. Environ. Sci. Technol. (2016) 13:2797–2804

Chen F, Zou W, Qu W, Zhang J (2009) Photocatalytic performance of a visible light TiO$_2$ photocatalyst prepared by a surface chemical modification process. Catal Commun 10:1510–1513

Chen Y, Huang G-F, Huang W-Q, Zou BS, Pan AL (2012) Enhanced visible-light photoactivity of La-doped ZnS thin films. Appl Phys A 108:895–900

Dein AME, Libra JA, Wiesmann U (2003) Mechanism and kinetic model for the decolorization of the azo dye reactive black 5 by hydrogen peroxide and UV radiation. Chemosphere 52:1069–1077

Ensing B, Buda F, Baerends EJJ (2003) Fenton-like chemistry in water: oxidation catalysis by Fe(III) and H$_2$O$_2$. Phys Chem 107:5722–5731

Gonzaleza MG, Oliveros E, Worner M, Braun AM (2004) Vacuum-ultraviolet photolysis of aqueous reaction systems. J Photochem Photobiol, C 5:225–246

Kim JP, Davidson MR, Holloway PHJ (2003) Improved brightness and efficiency in Ce codoped ZnS:TbOF electroluminescent thin films. J Appl Phys 93:9597–9603

Kummerer K (2009) Antibiotics in the aquatic environment. Chemosphere 75:417–434

Kuppayee M, Nachiyar GKV, Ramasamy V (2011) Synthesis and characterization of Cu^{2+} doped ZnS nanoparticles using TOPO and SHMP as capping agents. Appl Surf Sci 257:6779–6786

Masarwa A, Calis SR, Meyerstein N, Meyerstein D (2005) Oxidation of organic substrates in aerated aqueous solutions by the Fenton reagent. Coord Chem Rev 249:1937–1943

Muruganandham M, Suri RPS, Jafari S, Sillanpää M, Lee G-J, Wu JJ, Swaminathan M (2014) Recent developments in homogeneous advanced oxidation processes for water and wastewater treatment. Int J Photoenergy 2014:821674. doi:10.1155/2014/821674

Palominos RA, Mondaca MA, Giraldo A, Peñuela G, Pérez-Moya M, Mansilla D (2009) Photocatalytic oxidation of the antibiotic tetracycline on TiO$_2$ and ZnO suspensions. Catal Today 144:100–105

Pei D, Luan J (2012) Development of visible light-responsive sensitized photocatalysts. Int J Photoenergy 2012:262831. doi:10.1155/2012/262831

Peyton GR, Glaze WH (1988) Destruction of pollutants in water with ozone in combination with ultraviolet radiation. 3. Photolysis of aqueous ozone. Environ Sci Technol 22:761–767

RemaDevi BS, Raveendran R, Vaidyan AV (2007) Synthesis and characterization of Mn^{2+}-doped ZnS nanoparticles. Pramana J Phys 68:679–687

San N, Hatipoglu A, Koçtürk G, Çınar Z (2001) Prediction of primary intermediates and the photodegradation kinetics of

3-aminophenol in aqueous TiO$_2$ suspensions. J Photochem Photobiol, A 139:225–232

Singla P, Pandey OP, Singh K (2016) Study of photocatalytic degradation of environmentally harmful phthalate esters using Ni-doped TiO$_2$ nanoparticles. Int J Environ Sci Technol 13:849–856

Sivakumar P, Kumar GKG, Renganathan S (2014) Synthesis and characterization of ZnS–Ag nanoballs and its application in photocatalytic dye degradation under visible light. J Nanostruct Chem 4:107. doi:10.1007/s40097-014-0107-0

Tehrani-Bagha AR, Mahmoodi NM, Menger FM (2010) Degradation of a persistent organic dye from colored textile wastewater by ozonation. Desalination 260:34–38

Thuy UTD, Liema NQ, Parlett CMA, Lalev GM, Wilson K (2014) Synthesis of CuS and CuS/ZnS core/shell nanocrystals for photocatalytic degradation of dyes under visible light. Catal Commun 44:62–67

Vanini LS, Hirata TA, Kwiatkowski A, Clemente E (2009) Extraction and stability of anthocyanins from the Benitaka grape cultivar (Vitis vinifera L.). Braz J Food Technol 12(3):213–219. doi:10.4260/BJFT2009800900015

Verma B, Headley JV, Robarts RD (2007) Behaviour and fate of tetracycline in river and wetland waters on the Canadian Northern Great Plains. J Environ Sci Health A 42:109. doi:10.1080/10934520601011163

Westwood D (2007) The determination of chemical oxygen demand in waters and effluents. http://www.mwa.co.th/download/file_upload/SMWW_4000-6000.pdf

Yang P, Lu M, Xu D, Yuan D, Song C, Zhou G (2001) The effect of Co^{2+} and Co^{3+} on photoluminescence characteristics of ZnS nanocrystallines. J Phys Chem Solids 62:1181–1184

Yang P, Lu M, Xu D, Yuan D, Song C, Liu S, Cheng X (2003) Characteristics of ZnS nanoparticles co-doped with Ni^{2+} and Mn^{2+}. Opt Mater Lumin 24:497–502

Zhang J, Yu JG, Zhang YM, Li Q, Gong JR (2011) Visible light photocatalytic H$_2$-production activity of CuS/ZnS porous nanosheets based on photoinduced interfacial charge transfer. Nano Lett 11:4774–4779

Zhao Q, Xie Y, Zhang Z, Bai X (2007) Size-selective synthesis of zinc sulfide hierarchical structures and their photocatalytic activity. Cryst Growth Des 7:153–158

Zhiyu W, Haifeng C, Peisong T, Weiping M, Fuan Z, Guodong Q, Xianping F (2006) Hydrothermal in situ preparation of the copper phthalocyanine tetrasulfonate modified titanium dioxide photocatalyst. Colloids Surf A 289:207–211